arXiv:1406.4876v1 [astro-ph.GA] 18 Jun 2014

Fluorine in the solar neighborhood - is it all produced in AGB-stars?

H. Jönsson and N. Ryde
Lund Observatory, Department of Astronomy and Theoretical Physics, Lund University, Box 43, SE-221 00 Lund, Sweden
henrikj@astro.lu.se

G. M. Harper
School of Physics, Trinity College, Dublin 2, Ireland

M. J. Richter
Physics Department, University of California, Davis, CA 95616, USA
and

K. H. Hinkle
National Optical Astronomy Observatory, P.O. Box 26732, Tucson, AZ 85726, USA

ABSTRACT

The origin of 'cosmic' fluorine is uncertain, but there are three proposed production sites/mechanisms: AGB stars, ν nucleosynthesis in Type II supernovae, and/or the winds of Wolf-Rayet stars. The relative importance of these production sites has not been established even for the solar neighborhood, leading to uncertainties in stellar evolution models of these stars as well as uncertainties in the chemical evolution models of stellar populations.

We determine the fluorine and oxygen abundances in seven bright, nearby giants with well-determined stellar parameters. We use the 2.3 μm vibrational-rotational HF line and explore a pure rotational HF line at 12.2 μm. The latter has never been used before for an abundance analysis. To be able to do this we have calculated a line list for pure rotational HF lines. We find that the abundances derived from the two diagnostics agree.

Our derived abundances are well reproduced by chemical evolution models *only* including fluorine production in AGB-stars and therefore we draw the conclusion that this might be the main production site of fluorine in the solar neighborhood. Furthermore, we highlight the advantages of using the 12 μm HF lines to determine the possible contribution of the ν-process to the fluorine budget at low metallicities where the difference between models including and excluding this process is dramatic.

Subject headings: stars: abundances — solar neighborhood — molecular data

1. Introduction

'Cosmic' production of fluorine is difficult because fluorine is very easily destroyed in stellar interiors and therefore has to be deposited into the interstellar medium soon after its production. Because of this sensitivity to the conditions of its production site, the 'cosmic' fluorine abundance will not only put a severe constraint on the chem-

ical evolution models describing different stellar populations, but also on stellar evolution models.

Three production sites/mechanisms have been proposed to contribute to the 'cosmic' fluorine abundance: thermal-pulsing asymptotic giant branch (TP-AGB) stars, ν nucleosynthesis in supernovae type II (SNeII), and/or Wolf-Rayet (W-R) stars (see Jönsson et al. (2014) for further details). So far, only the production of fluorine in AGB-stars has been proven by observations: by direct measurements of fluorine abundance in AGB-stars (Jorissen et al. 1992; Abia et al. 2009, 2010), by measurements of fluorine in post AGB-stars and planetary nebulae (Werner et al. 2005; Zhang & Liu 2005; Otsuka et al. 2008) as well as in carbon-enhanced metal-poor stars (Schuler et al. 2007; Lucatello et al. 2011), and in Ba-stars (Alves-Brito et al. 2011). Also fluorine pollution by AGB-stars in globular clusters has been shown by for example D'Orazi et al. (2013). When it comes to the production of fluorine by the ν-process, Federman et al. (2005) do not see any evidence for it in the interstellar medium and the fluorine production of W-R stars has been theoretically questioned by Palacios et al. (2005). This means that these two production sites are more speculative at the moment.

To determine the relative role of the three production processes more observations are needed. However, determining the fluorine abundance is not easy because of a lack of spectral lines in stellar spectra. The HF line at 2.3 μm is often used, but it is very weak in dwarfs and metal-poor giants. Unfortunately it is situated in a region with a lot of telluric lines adding even more uncertainty to the fluorine abundance determined from this line (de Laverny & Recio-Blanco 2013). Furthermore there have been several sets of molecular data for the HF molecule used in the literature: one from Jorissen et al. (1992), in turn from Tipping and one from Decin (2000), in turn from Sauval, differing in the excitation energy by 0.25 eV. For further details on these line lists, see Jönsson et al. (2014), where a HF line list compatible with the partition function built into many spectral synthesis programs (for example MOOG, BSYN, and SME) was presented. Shortly thereafter Maiorca et al. (2014) published a version of the HF line list based on Einstein A-values from the HITRAN2012 database. These A-values are very close to the values used in Jönsson et al. (2014) leading to an agreement of the loggf values within $\sim$0.01 dex.

When it comes to fluorine production in the solar neighborhood, as mentioned earlier, Jorissen et al. (1992) and Abia et al. (2009, 2010) showed production in AGB-stars. Recio-Blanco et al. (2012) argued that the main production site is AGB-stars, while Nault & Pilachowski (2013) claim that the relative fluorine contribution from AGB-stars probably are *not* the main source of fluorine in the solar neighborhood, but rather the ν-process. In line with the modeling of Kobayashi et al. (2011a), who predict that the largest difference in fluorine abundance for a scenario with and without the ν-process can be found in metal-poor stars, Li et al. (2013) explore metal-poor field giants, and show that neither model fit their observations well. However, the model closest to the observed values is the one including the ν-process.

Obviously the question of the fluorine abundance trend in the solar neighborhood is still open, and there is indeed need for further study.

In this *Letter*, we reevaluate the chemical evolution of fluorine in the solar neighborhood by comparing current models with newly derived fluorine abundances for seven bright giants using our new line lists, including the HF lines around 12 μm, which are here used for the first time. The 12.2 μm line used is much stronger than the 2.3 μm line and is not affected by telluric lines.

2. Observations

Spectra of seven bright, nearby giants in the 12.2 μm region were recorded with the spectrometer TEXES (Lacy et al. 2002) mounted on IRTF on Mauna Kea during 2000, 2001 and 2006. The spectra were extracted and reduced in a typical manner (see Lacy et al. (2002) for further details) and have a resolution of R $\sim$65,000 and a signal-to-noise ratio of typically 100. Furthermore, we have retrieved four spectra covering the 2.3 μm HF line observed with the FTS mounted on the Kitt Peak National Observatory Mayall 4 m reflector (one of the four spectra is the IR Arcturus atlas by Hinkle et al. (1995)). These observations were made on June, 24 1977, August, 24 1983, and on April, 13 1990. For the determinations of metallicity and oxygen abundances, we searched spectral

archives for visual spectra of our target stars and found three from the NARVAL spectrometer, one from HARPS (Mayor et al. 2003), and one from ELODIE (Baranne et al. 1996).

3. Analysis

All spectra were analyzed using the software `Spectroscopy Made Easy`, SME (Valenti & Piskunov 1996) and a grid of MARCS spherical symmetric LTE models (Gustafsson et al. 2008).

3.1. Stellar parameters

The stellar parameters used are listed in Table 1. Effective temperatures determined from angular diameter measurements are taken from Mozurkewich et al. (2003), and gravities are determined from the stellar radius (Mozurkewich et al. 2003), the parallax (van Leeuwen 2007), and fits to evolutionary tracks (see Ryde et. al (in prep.) for further description). The [Fe/H] and the optical microturbulence were, for five of our stars, determined from Fe I-lines in visual spectra from the three different spectroscopical archives. For the remaining two stars we could not find any optical spectra, but use literature values for the metallicity, see Table 1. For the IR spectra we, as suggested by Tsuji (2008), instead use a slightly higher value of 2.0 km/s for the microturbulence for all stars.

Typical uncertainties of the stellar parameters are $\sigma T_{\rm eff}$=50 K, $\sigma \log g$=0.1, σ[Fe/H]=0.1, and $\sigma v_{\rm mic}$=0.5 kms^{-1}.

3.2. Line data

The line data for all lines used are the same as in Jönsson et al. (2014), except for the HF line at 12.2 μm. We use the partition function already presented in Jönsson et al. (2014), which is an updated version of the one from Sauval & Tatum (1984). Since Equation 3 in Jönsson et al. (2014) is not entirely correct, we give it here again, see below. The Figure 2 shown in Jönsson et al. (2014) is however correct. The partition function is given by $\ln Q = \sum_{i=0}^{5} a_i \times (\ln T[\mathrm{K}])^i$ where

$$\mathbf{a} = \begin{pmatrix} -360.544650 \\ 222.384130 \\ -54.5664753 \\ 6.69351087 \\ -0.409637436 \\ 0.0100497602 \end{pmatrix}$$

The excitation energies were computed from the energy-level expression and coefficients of Leblanc et al. (1994). The transition frequencies were calculated from the differences of the energy levels involved in the transition, and agree excellently with accurately measured frequencies from Jennings et al. (1987). The HF Einstein decay coefficients, A_{ji}, for the rotational transitions were computed using the accurate dipole moment found by Muenter & Klemperer (1970). The oscillator strengths, the gf values, were then calculated with the conversion given in Larsson (1983). We used a statistical weight following our partition function, $g = 2J + 1$, where J is the rotational quantum number. Our calculated data for the rotational HF lines are listed in Table 2.

3.3. Stellar abundances

The iron abundances were determined from optical Fe I-lines or taken from literature sources (see Section 3.2 and Table 1). The oxygen abundances were determined from the FTS spectra using OH-lines around 1.56 μm, and when optical archive spectra were available, also from the [O I] line at 6300 Å. The final oxygen abundance used in Figures 2-3 is the mean value of these two. For four of our stars we have FTS K-band spectra where the 2.3 μm HF line is unaffected by telluric lines, so for that subset of stars we are able to compare the fluorine abundances as derived from the 12.2 μm HF line to the abundances from the 2.3 μm line. To our knowledge this is the first determination of fluorine for all stars presented here except αBoo, which has been extensively studied because of the available atlas of Hinkle et al. (1995). For example Nault & Pilachowski (2013) get a value of A(F)= 3.75 from the 2.3 μm line, which is close to our value[1].

The uncertainties in the determined abun-

[1] Nault & Pilachowski (2013) use the line list of Sauval, which is very similar to to our, and MOOG, which is distributed with a partition function compatible with these lists, so our abundance results most likely are on the same scale.

Table 1

Stellar parameters and abundances for our program stars.

Star	HD	$T_{\rm eff}$	logg	[Fe/H][a]	$v_{\rm mic}$[b]	$v_{\rm mic}$[c]	$A({\rm O})_{\rm [OI]}$	$A({\rm O})_{\rm OH}$	$A({\rm O})_{\rm mean}$	$A({\rm F})_{2.3\mu}$	$A({\rm F})_{12.2\mu}$
δVir	112300	3602	0.84	-0.14[2]	···	2.00	···	8.65	8.65	···	4.20
δOph	146051	3721	1.02	-0.24[e]	1.48[e]	2.00	8.48[e]	8.53	8.50	4.02	4.04
μUMa	89758	3793	1.07	-0.34[f]	1.66[f]	2.00	8.47[f]	8.43	8.45	3.94	4.05
αLyn	80493	3836	0.98	-0.31[1]	···	2.00	···	···	···	···	3.96
αTau	29139	3871	1.27	-0.25[d]	1.51[d]	2.00	8.57[d]	8.53	8.55	4.16	4.34
αHya	81797	4060	1.35	-0.17[d]	1.84[d]	2.00	8.62[d]	8.54	8.58	···	4.12
αBoo	124897	4226	1.67	-0.62[d]	1.65[d]	2.00	8.60[d]	8.40	8.50	3.65	3.73

[a]We use A(Fe)$_\odot$=7.50 (Asplund et al. 2009).

[b]microturbulence used for the visual spectra.

[c]microturbulence used for the IR spectra.

[d]As determined from NARVAL archive spectrum.

[e]As determined from FEROS archive spectrum.

[f]As determined from ELODIE archive spectrum.

References. — (1) McWilliam (1990); (2) Smith & Lambert (1985)

Table 2

HF rotational transitions[a].

J'	J''	σ [cm^{-1}]	$\lambda_{\rm air}$ [Å]	$\chi_{exc,low}$ [cm^{-1}]	$\chi_{exc,low}$ [eV]	$A_{J',J''}$ [s^{-1}]	$\log gf$
1	0	41.111	2431777.1601	0.00	0.000	0.024	-4.191
2	1	82.171	1216640.9581	41.11	0.005	0.232	-3.589
3	2	123.130	811930.5537	123.28	0.015	0.837	-3.237
4	3	163.936	609827.2819	246.41	0.031	2.049	-2.988
5	4	204.540	488767.6306	410.35	0.051	4.070	-2.795
6	5	244.893	408230.6151	614.89	0.076	7.092	-2.637
7	6	284.944	350850.2607	859.78	0.107	11.296	-2.505
8	7	324.646	307943.7237	1144.73	0.142	16.847	-2.390
9	8	363.951	274687.3322	1469.37	0.182	23.893	-2.289
10	9	402.812	248187.0031	1833.32	0.227	32.564	-2.199
11	10	441.184	226601.1585	2236.14	0.277	42.971	-2.118
12	11	479.021	208702.1853	2677.32	0.332	55.203	-2.045
13	12	516.281	193640.2976	3156.34	0.391	69.325	-1.978
14	13	552.920	180808.6018	3672.62	0.455	85.383	-1.916
15	14	588.899	169762.1355	4225.54	0.524	103.397	-1.858
16	15	624.177	160167.2678	4814.44	0.597	123.363	-1.805
17	16	658.717	151768.9583	5438.62	0.674	145.254	-1.755
18	17	692.481	144368.9299	6097.33	0.756	169.024	-1.709
19	18	725.435	137810.7354	6789.81	0.842	194.598	-1.665
20	19	757.545	131969.3039	7515.25	0.932	221.884	-1.624
21	20	788.780	126743.4749	8272.80	1.026	250.769	-1.585
22	21	819.109	122050.5681	9061.58	1.123	281.119	-1.549
23	22	848.504	117822.3714	9880.69	1.225	312.785	-1.514
24	23	876.938	114002.1308	10729.19	1.330	345.601	-1.481
25	24	904.385	110542.2649	11606.13	1.439	379.388	-1.450

[a]The consistent partition function is given in the text.

dances from the uncertainties in the stellar parameters (see Section 3.2) are generally small with σA(O)= 0.1, $\sigma A(\mathrm{F})_{2.3\mu} = 0.1$, and $\sigma A(\mathrm{F})_{12.2\mu} = 0.2$. The 2.3 μm line is more temperature sensitive than the 12.2 μm HF line and, for our sample of stars, the 12.2 μm HF line is typically very sensitive to the microturbulence, the reason being that it is on the verge of being saturated for most of our stars ($\log W_\lambda/\lambda \geq -5.3$).

In Figure 1 we show the spectra around the 12.2 μm HF line for our stars. We note that the HF-line is blended with a Mg I line (122051.12 Å, $\chi_{exc,low} = 7.092$, and $\log gf = 0.353$), but assuming the atomic data is correct (it is rated 'B+' in the NIST database, meaning an uncertainty in the transition probability of $\leq 7\%$) SME will compensate for this line in the spectral fitting and the fluorine abundance determination. Several water lines are also present in the 12 μm region, which will be explored in a forthcoming paper (Ryde et al. in prep).

4. Results and discussion

Our abundance results are listed in Table 1 and plotted in Figures 2-3. The fluorine abundances as derived from the 2.3 μm line and the 12.2 μm line are in close agreement for all stars except αTau where the latter value is $\sim$0.2 dex higher than the former. However, because of the strong microturbulence dependence of the 12.2 μm line this is within the uncertainties. We note that changing the IR microturbulence, within the uncertainty, to 2.5 km/s will shift this value into the trends of the others in the plots.

Since the fluorine abundances derived from the 2.3 μm and the 12.2 μm lines agree so well using standard MARCS atmospheres for these red giants, we can conclude that also the formation of the 12 μm lines are well described by such models. On the contrary, numerous water lines in this wavelength region are poorly modelled. Ryde et al. (2002, 2006) thus constructed a semi-empirical model atmosphere which could explain the formation of strong water lines. A cooling of the outer atmosphere of a few 100 K, at $\log \tau_{500} < -4$, was needed. This extra outer cooling does, however, not significantly affect the 12.2 μm HF line, since it is formed deeper in the photosphere: the derived fluorine abundance is only 0.07 dex higher for αBoo when using a standard MARCS model compared to using the modified MARCS model of Ryde et al. (2002).

Available chemical evolution models of fluorine in the solar neighborhood predict very similar abundance trends. In Figures 2-3 we have chosen to compare our results to the chemical evolution models of Kobayashi et al. (2011b) since those are the only models to our knowledge showing the evolution of fluorine from production in only AGB-stars. For example the models of Renda et al. (2004) have chemical evolution models of fluorine including (i) the ν-process, (ii) the ν-process and W-R stars, and (iii) ν-process, W-R stars and AGB-stars. Since AGB-stars are the only source of fluorine that has been observationally proven (see Section 1) we find the combinations of chemical models in Kobayashi et al. (2011b) to be more appropriate: they have one including fluorine production only in AGB-stars and two including fluorine production in AGB-stars *and* two different ν-process energies.

From the left panel of Figure 2, two observations can be made: first, the models *only* including the AGB star contribution seem to predict the fluorine production compared to iron well within uncertainties, and second, almost all our [F/Fe]-values are slightly sub-solar. The second observation might suggest that the solar value used ($\mathrm{A(F)}_\odot = 4.40$ taken from Maiorca et al. (2014)) is too high or that some other process is present. We note, however, that taking the large uncertainty of the solar value (σA(F)= 0.25) into account, our observed trend is in good agreement with the solar value. It would be desirable to determine the solar fluorine abundance to a higher accuracy. However, none of the spectral lines published here or in Jönsson et al. (2014) below 22 μm are visible in the photospheric solar atlases of Hase et al. (2010) and Wallace et al. (1994). A general estimation of the line strength by $\mathrm{gf} \cdot e^{-\chi_{\mathrm{exc}}/kT}$ shows that the lines above 22 μm will only get weaker, meaning that when determining the solar fluorine abundance spectroscopically, one has to use a spectrum from a sunspot. Large uncertainties like the above are then expected because of the uncertainty of the temperature in, and the modeling of, the sunspot.

From the right panel of Figure 2 we see that αBoo (the most metal-poor star in our sample)

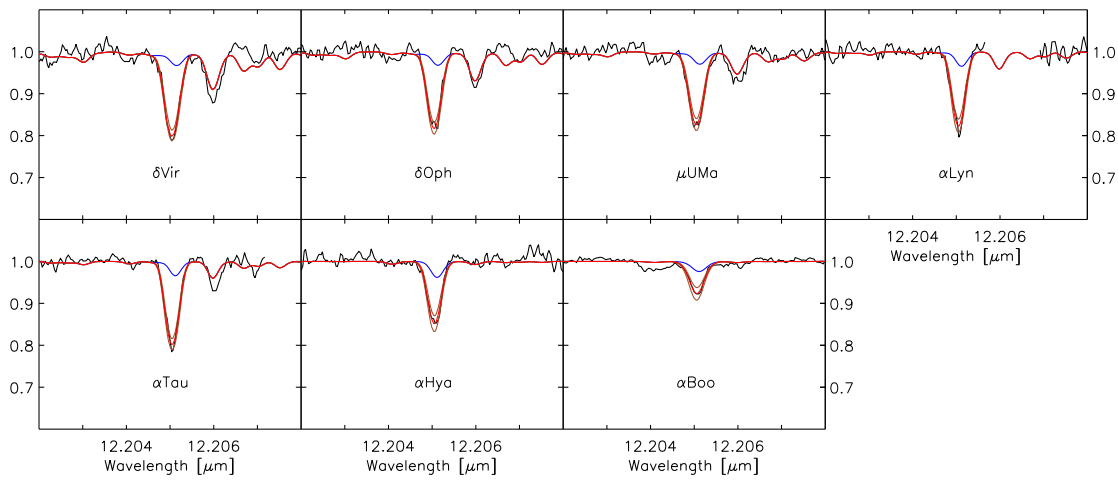

Fig. 1.— Spectra showing the 12.2 μm HF line for our stars. Our best fit is shown in red and ± 0.2 dex is shown in brown. Note that the best fit is determined by χ^2-minimization and simply comparing the synthetic spectra to the observed by eye would most probably lead to higher abundances for αLyn and αTau. The contribution of the blending Mg I line is shown in blue. All other lines are due to water and we note that some of them are not well reproduced in the synthetic spectra of the coolest stars. This will be explored in a future paper (Ryde et al. in prep).

has an oxygen abundance most consistent with it being of thick disk-type (this is explored in much more detail in Ramírez & Allende Prieto (2011)). In the left panel it is indeed slightly better fitted by the thick disk model than the solar neighborhood model, but both models predict higher fluorine than we measure.

In Figure 3, we plot [F/O] vs [O/H] to exclude the iron dependence and to better distinguish between contributions from SNIIe and AGB-stars, since iron is abundantly produced in type Ia SNe. We see that the chemical evolution model only including AGB-stars and excluding the ν-process (Kobayashi et al. 2011a) best reproduce our fluorine and oxygen abundances. One star, αBoo, falls below the line of the solar neighborhood model, but on the other hand, in this case, it is well reproduced by the thick disk model. The uncertainties of our data in Figure 3 only give room for a ν-process with a neutrino energy much lower than expected (Hartmann et al. 1991), which corroborates the results of Li et al. (2013).

Based on the combination of Figures 2-3, our small sample of stars seem to show that only AGB-stars are needed to explain the fluorine abundance in the solar neighborhood. Eventhough the AGB-star and the ν-process contributions are of similar order in the relatively short metallicity range of our observations (Renda et al. 2004), including both in the models would most likely overpredict the fluorine abundance. It should, however, be noted that there are certainly uncertainties in these models, and they depend, to different degrees, on uncertain input values. Therefore, to draw firm conclusions, more observations would be needed: ideally more metal-poor stars to even better test the presence or not of the ν-process, and more metal-rich stars to test the possible production of fluorine in W-R stars. As stated earlier, the 2.3 μm HF line becomes too weak in metal-poor stars, but the 12.2 μm line, that is strong in our sample of stars, should be well suited to use for abundance determinations as low as [Fe/H]~ -2. Also further galactic chemical evolution modeling including fluorine production in W-R stars, SNeII and AGB stars together, in different combinations, and independently would be helpful in trying to determine the major contributor of fluorine in the solar neighborhood.

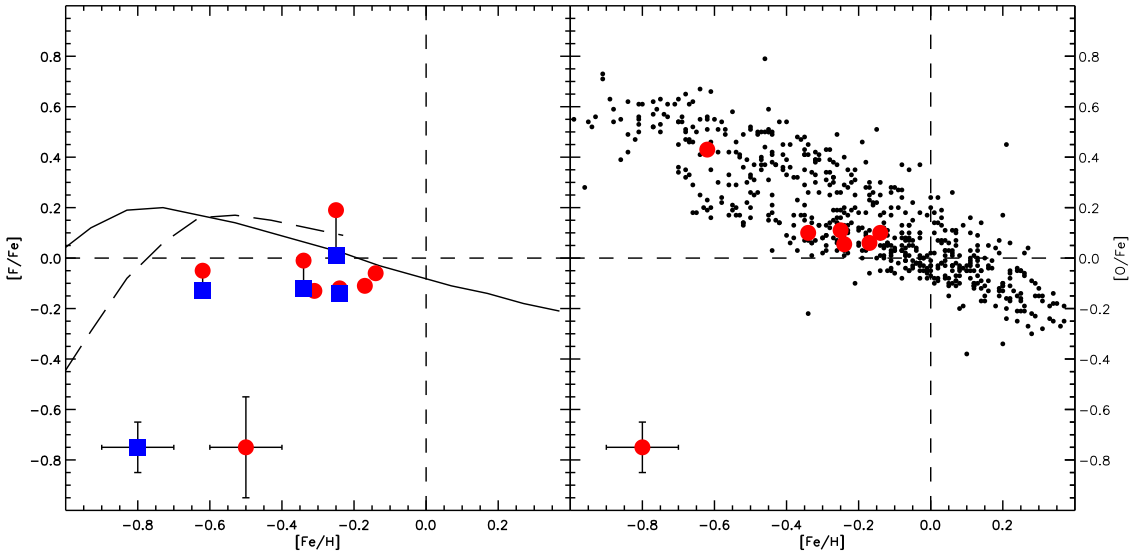

Fig. 2.— [F/Fe] and [O/Fe] as functions of [Fe/H] for our program stars. Left panel: results from the 2.3 μm HF line are marked with blue squares and results from the 12.2 μm line are marked with red dots. Results for the same stars are interlinked with lines. Also shown are the predictions of the models from Kobayashi et al. (2011b) not including fluorine production in W-R stars and via the ν-process. The full line is the solar neighborhood model and the dashed line is the thick disk model. The model predictions have been transformed to the solar abundance scale of A(F)$_\odot$=4.40 (Maiorca et al. 2014) and A(Fe)$_\odot$=7.50 (Asplund et al. 2009). Right panel: the oxygen abundances plotted are the mean of the abundances derived from the 6300 Å [O I]-line and 1.55 μm OH-lines. The black dots are the solar neighborhood dwarfs of Bensby et al. (2014) consisting of thin- and thick disk type stars showing the typical bi-modality of lower and higher oxygen enhancement, respectively. Conservative estimates of the uncertainties are marked in the lower left corners in both panels.

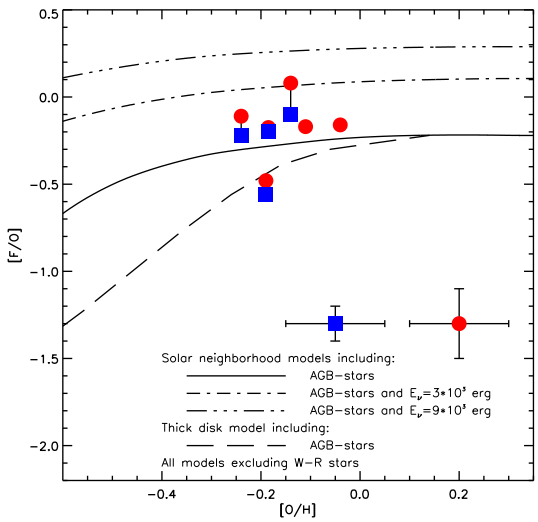

Fig. 3.— Our fluorine abundances compared with the predictions of the models from Kobayashi et al. (2011a) and Kobayashi et al. (2011b). The model predictions have been transformed to the solar abundance scale of $A(F)_\odot$=4.40 (Maiorca et al. 2014) and $A(O)_\odot$=8.69 (Asplund et al. 2009). Results from the 2.3 μm HF line are marked with blue squares and results from the 12.2 μm line are marked with red dots. Results for the same stars are interlinked with lines. Conservative estimates of the uncertainties are marked above the text in the plot.

5. Conclusions

We present a new line list, with excitation energies and lines strengths, for N-band HF lines and for the first time use one of them for fluorine abundance determination. The abundances derived from this line agrees with the abundances derived from the often used 2.3 μm line, within uncertainties, for our sample of stars. Thus, our HF lines list for the vibration-rotation lines as presented in Jönsson et al. (2014) and that for the pure rotational lines in the N band presented here, give consistent results.

Our measured fluorine-oxygen abundance trend suggests that the fluorine production in AGB-stars might be sufficient to explain the fluorine abundance in the solar neighborhood and that the ν-process is not needed. However, to firmly establish this, more observations are needed. Since the 2.3 μm line is very weak in metal-poor stars and the N-band lines are much stronger, these lines can probably help determining the possible significance of the ν-process in the chemical evolution of the solar neighborhood.

Kjell Eriksson is thanked for generous help with the modified MARCS model, and the anonymous referee is thanked for insightful comments that helped improve this *Letter* in several ways. This research has been supported by the Royal Physiographic Society in Lund, Stiftelsen Walter Gyllenbergs fond. This research draws upon data as distributed by the NOAO Science Archive. NOAO is operated by the Association of Universities for Research in Astronomy (AURA) under cooperative agreement with the National Science Foundation. This publication made use of the SIMBAD database, operated at CDS, Strasbourg, France, NASA's Astrophysics Data System, and the VALD database, operated at Uppsala University, the Institute of Astronomy RAS in Moscow, and the University of Vienna.

Facilities: IRTF (TEXES), Mayall (FTS), ESO:3.6m (HARPS), TBL (NARVAL), OHP:1.93m (ELODIE).

REFERENCES

Abia, C., Recio-Blanco, A., de Laverny, P., et al. 2009, ApJ, 694, 971

Abia, C., Cunha, K., Cristallo, S., et al. 2010, ApJL, 715, L94

Alves-Brito, A., Karakas, A. I., Yong, D., Meléndez, J., & Vásquez, S. 2011, A&A, 536, 40

Asplund, M., Grevesse, N., Sauval, A. J., & Scott, P. 2009, ARA&A, 47, 481

Baranne, A., Queloz, D., Mayor, M., et al. 1996, A&AS, 119, 373

Bensby, T., Feltzing, S., & Oey, M. S. 2014, A&A, 562, 71

de Laverny, P., & Recio-Blanco, A. 2013, A&A, 560, 74

Decin, L. 2000, PhD thesis, 16

D'Orazi, V., Lucatello, S., Lugaro, M., et al. 2013, ApJ, 763, 22

Federman, S. R., Sheffer, Y., Lambert, D. L., & Smith, V. V. 2005, ApJ, 619, 884

Gustafsson, B., Edvardsson, B., Eriksson, K., et al. 2008, A&A, 486, 951

Hartmann, D. H., Haxton, W. C., Hoffman, R. D., & Woosley, S. E. 1991, NuPhA, 527, 663

Hase, F., Wallace, L., McLeod, S. D., Harrison, J. J., & Bernath, P. F. 2010, JQSRT, 111, 521

Hinkle, K., Wallace, L., & Livingston, W. C. 1995, San Francisco, Calif. Astronomical Society of the Pacific

Jennings, D. A., Evenson, K. M., Zink, L. R., et al. 1987, JMoSp, 122, 477

Jönsson, H., Ryde, N., Harper, G. M., et al. 2014, A&A, 564, 122

Jorissen, A., Smith, V. V., & Lambert, D. L. 1992, A&A, 261, 164

Kobayashi, C., Izutani, N., Karakas, A. I., et al. 2011a, ApJL, 739, L57

Kobayashi, C., Karakas, A. I., & Umeda, H. 2011b, MNRAS, 414, 3231

Lacy, J. H., Richter, M. J., Greathouse, T. K., Jaffe, D. T., & Zhu, Q. 2002, PASP, 114, 153

Lambert, J., Josselin, E., Ryde, N., & Faure, A. 2013, EAS Publications Series, 60, 111

Larsson, M. 1983, A&A, 128, 291

Leblanc, R. B., White, J. B., & Bernath, P. F. 1994, JMoSp, 164, 574

Li, H. N., Ludwig, H. G., Caffau, E., Christlieb, N., & Zhao, G. 2013, ApJ, 765, 51

Lucatello, S., Masseron, T., Johnson, J. A., Pignatari, M., & Herwig, F. 2011, ApJ, 729, 40

Maiorca, E., Uitenbroek, H., Uttenthaler, S., et al. 2014, ApJ, 788, 149

Mayor, M., Pepe, F., Queloz, D., et al. 2003, The Messenger (ISSN0722-6691), 114, 20

McWilliam, A. 1990, ApJS, 74, 1075

Mozurkewich, D., Armstrong, J. T., Hindsley, R. B., et al. 2003, AJ, 126, 2502

Muenter, J. S., & Klemperer, W. 1970, JChPh, 52, 6033

Nault, K. A., & Pilachowski, C. A. 2013, AJ, 146, 153

Otsuka, M., Izumiura, H., Tajitsu, A., & Hyung, S. 2008, ApJ, 682, L105

Palacios, A., Arnould, M., & Meynet, G. 2005, A&A, 443, 243

Ramírez, I., & Allende Prieto, C. 2011, ApJ, 743, 135

Recio-Blanco, A., de Laverny, P., Worley, C., et al. 2012, A&A, 538, 117

Renda, A., Fenner, Y., Gibson, B. K., et al. 2004, MNRAS, 354, 575

Ryde, N., Harper, G. M., Richter, M. J., Greathouse, T. K., & Lacy, J. H. 2006, ApJ, 637, 1040

Ryde, N., Lambert, D. L., Richter, M. J., & Lacy, J. H. 2002, ApJ, 580, 447

Sauval, A. J., & Tatum, J. B. 1984, ApJS (ISSN 0067-0049), 56, 193

Schuler, S. C., Cunha, K., Smith, V. V., et al. 2007, ApJ, 667, L81

Smith, V. V., & Lambert, D. L. 1985, ApJ, 294, 326

Tsuji, T. 2008, A&A, 489, 1271

Valenti, J. A., & Piskunov, N. 1996, A&AS, 118, 595

van Leeuwen, F. 2007, A&A, 474, 653

Wallace, L., Livingston, W., & Bernath, P. 1994, NSO Technical Report

Werner, K., Rauch, T., & Kruk, J. W. 2005, A&A, 433, 641

Zhang, Y., & Liu, X. W. 2005, ApJ, 631, L61

This 2-column preprint was prepared with the AAS LaTeX macros v5.2.